PHYSICAL REVIEW D VOLUME 19, NUMBER 5 1 MARCH 1979

Effective potential for heavy-quark–antiquark bound systems

Robert Levine and Yukio Tomozawa
The Harrison M. Randall Laboratory of Physics, University of Michigan, Ann Arbor, Michigan 48109
(Received 5 October 1978)

An analytic form for the quark-antiquark interaction potential is proposed based on the renormalization-group equation of quantum chromodynamics (QCD) and the confinement assumption. With validity of the nonrelativistic approximation assumed, energy spectra, leptonic decay width, and $E1$ transition rates are computed. The results are compared with experimental data of ψ and Υ resonances. A possible spin-spin interaction of non-QCD origin is then discussed.

I. INTRODUCTION

Many seemingly unconnected theories have grown out of SU(3) color gauge theory [quantum chromodynamics (QCD)]. These include asymptotically free (and renormalization-group), confinement, and instanton theories. The possibility of combining them within a single experimentally verifiable framework appeared with the discovery of the ψ/J and Υ particles.

There have been various attempts to understand the ψ/J and Υ systems in terms of a quark-antiquark nonrelativistic potential.[1-6] Although gross features of the systems have been explained in this way, the problem of connecting the potential with QCD remains.

Recently, in an interesting article, Celmaster and Henyey[5] proposed an approximation scheme which incorporates the asymptotically free expansion of the renormalization-group equation and current linear-confinement assumptions. Using the renormalization-group equation they obtained the potential from a numerical integration of the running coupling constant.[7] Then they calculated the $1S$-$2S$ energy-split dependence on quark mass. Since this is a reasonable approach, we have attempted to derive an analytic form for the potential within their scheme and then use this to analyze ψ/J and Υ data in more detail. In another direction, the failure of the relativistic QCD potential to explain the observed splitting of the singlet and triplet S states led Wilczek and Zee[8] to suggest a large spin-spin interaction due to instantons. This interaction should be part of a complete analysis and we will touch upon it in this article.

In Sec. II, we derive the analytic form for the potential based on the renormalization-group equation solution of Celmaster and Henyey. In Sec. III, we examine various ways of constructing the potential and determining parameters in the analytic form. These potentials are used to analyze experimental data and discuss results in Sec. IV. Finally, in Sec. V, the effect of a possible instanton spin-spin interaction is examined.

II. ANALYTIC FORM OF QCD POTENTIAL

The quark interaction potential is the Fourier transform of $\alpha(q^2)/q^2$ where $\alpha = g^2/4\pi$ is the running coupling constant.[9] This constant satisfies the renormalization-group equation[10]

$$\frac{d(\alpha/2\pi)}{d(\ln q^2)} = \frac{(\alpha)}{(2\pi)}\,\frac{\beta}{g}\,, \tag{2.1}$$

where

$$\frac{\beta}{g} = -b_1(\alpha/2\pi) - b_2(\alpha/2\pi)^2 + \cdots\,. \tag{2.2}$$

The coefficients b_1 and b_2 in the SU(3) gauge group are given by[11]

$$b_1 = (\tfrac{11}{2} - \tfrac{1}{3}N_f) \text{ and } b_2 = (\tfrac{51}{2} - \tfrac{19}{6}N_f)\,, \tag{2.3}$$

where N_f is the number of quark flavors. The condition of asymptotic freedom, $b_1 > 0$, then limits $N_f \leq 16$ and the above expansion corresponds to $q^2 \to \infty$. The behavior at $q^2 \to 0$ involves the confinement properties and, in particular, a linear potential corresponds to $\alpha \to A/q^2$ or $\beta/g \to -1$.

Following Celmaster and Henyey,[5] the behavior of β/g at $q^2 \to 0$ and $q^2 \to \infty$ is connected with a Padé approximation which results in the expression

$$\frac{d(\alpha/2\pi)}{d(\ln q^2)} = \frac{\alpha}{2\pi}\left[\frac{-b_1^2(\alpha/2\pi)(\alpha/2\pi + \alpha_0/2\pi)}{b_1^2(\alpha/2\pi)^2 + (b_2 - b_1\alpha_0/2\pi)\,\alpha/2\pi + b_1\alpha_0/2\pi}\right], \tag{2.4}$$

where $(\alpha_0/2\pi)$ is an arbitrary constant. Solving for q^2,

$$\frac{q^2}{\Lambda^2}=e^{2\pi/b_1\alpha}(\alpha_0/\alpha)[2/(1+\alpha_0/\alpha)]^{(1+b_2/b_1^2)}, \tag{2.5}$$

where Λ = an integration constant. The potential in coordinate space is given by

$$V(r)=\frac{-8}{3\pi}\int_0^\infty \alpha(q^2)\frac{\sin qr}{qr}dq. \tag{2.6}$$

In the limit $r\to\infty$,

$$V(r)\to\frac{r}{2\pi\alpha_R'(0)}. \tag{2.7}$$

For this limit $\alpha_R'(0)$ is defined as the slope of the Regge trajectories in the naive rotating-string model[5] $[\alpha_R'(0)\simeq 0.9\ \mathrm{GeV}^{-2}]$. This can be used to find a relationship between α_0 and Λ in (2.5) above. Taking $q^2\to 0$, (2.5) reduces to $\alpha=A/q^2$ which corresponds to[12] $V(r)=\frac{2}{3}$ Ar. Therefore, $A=3/4\pi\alpha_R'(0)$ and from (2.5) and the value of $\alpha_R'(0)$ we have

$$A=\Lambda^2\alpha_0 2^{(1+b_2/b_1^2)}=0.2652\ \mathrm{GeV}^2. \tag{2.8}$$

The remaining parameter (α_0 or Λ) can be determined from experimental data at a particular momentum.

In order to find an analytic form for the potential $V(r)$, we consider the asymptotic behavior of (2.5),

$$q^2\to\infty,\quad \alpha(q^2)=\frac{2\pi}{b_1\ln q^2}+\cdots, \tag{2.9}$$

$$\begin{aligned}&q^2\to 0,\quad \alpha(q^2)=A/q^2+\tilde\alpha(q^2),\\ &\tilde\alpha(q^2)=(B-Cq^2+\cdots),\end{aligned} \tag{2.10}$$

where

$$B=\frac{2\pi}{b_1}-(1+b_2/b_1^2)\alpha_0 \tag{2.11}$$

and

$$C=\frac{(2\pi)^2}{A}\frac{1}{2b_1^2}\left[1-2b_1(1+b_2/b_1^2)\frac{\alpha_0}{2\pi}+(1+b_2/b_1^2)b_2(\alpha_0/2\pi)^2\right]. \tag{2.12}$$

A simple analytic expression which interpolates between the two limits above is given by

$$\tilde\alpha(q^2)=\frac{2\pi}{b_1\ln(a+bq^2)}, \tag{2.13}$$

where

$$B=\frac{2\pi}{b_1}\frac{1}{\ln a} \tag{2.14}$$

and

$$\frac{C}{B}=\frac{b}{a\ln a}. \tag{2.15}$$

The potential in the asymptotic free region is obtained from Eqs. (2.9) and (2.6), and

$$V(r)=\frac{-8}{3\pi}\int_0^\infty\frac{2\pi}{b_1}\frac{1}{\ln q^2}\frac{\sin qr}{qr}dr. \tag{2.16}$$

With $x=qr$, we have

$$\begin{aligned}V(r)&=\frac{-8}{3\pi}\int_0^\infty\frac{2\pi}{b_1}\left[\frac{1}{\ln(1/r^2)+\ln x^2}\right]\frac{\sin x}{x}\frac{dx}{r}\\ &\xrightarrow[r\to 0]{}\frac{4}{3}\left(\frac{2\pi}{b_1}\frac{1}{r\ln r^2}\right).\end{aligned} \tag{2.17}$$

Using Eq. (2.13), we show in the Appendix that, for $r\to\infty$,

$$V(r)\to\tfrac{2}{3}Ar-\frac{4B}{3r}\left(1-2\ln a\sqrt{b/a}\,\frac{e^{-\sqrt{a/b}\,r}}{r(\ln r)^2}\right). \tag{2.18}$$

An interpolation between the two asymptotic limits as expressed in Eqs. (2.17) and (2.18) is given by

$$V(r)=\tfrac{2}{3}Ar-\tfrac{2}{3}\frac{2\pi}{b_1\ln(ke^{-\mu r}/r+d)}\frac{1}{r}, \tag{2.19}$$

where

$$B=\frac{\pi}{b_1\ln d}\quad\text{and}\quad \mu=\sqrt{a/b}. \tag{2.20}$$

For large r, the dependence of the argument of the logarithm in (2.19) is actually $[ke^{-\mu r}/r(\ln r)^2+d]$, however, we can neglect the variation of $\ln r$ and incorporate it into the constant k. The dominance of the linear term and exponential damping in the argument of the logarithm favor this simplification. Equations (2.18) and (2.19) are general in that different forms for $\tilde\alpha(q^2)$ correspond to the same $V(r)$ form with different parameters. For example,

$$\tilde\alpha(q^2)\propto 1/\ln\left(\prod_i(a_i+b_iq^2)\right)$$

corresponds to the form (2.19) with $\mu=\min_i[(a_i/b_i)^{1/2}]$ and $\tilde\alpha(q^2)\propto 1/\ln(a+bq^4)$ corresponds to $\mu=1/\sqrt{2}(a/b)^{1/4}$. Owing to this indeterminacy, we determined the parameters μ and k by numerical integration of the Fourier transform (2.6) using (2.5) at $r=0.5$ and $r=2.0$. The remaining parameter d depends only upon the number of flavor and the experimentally determined constant α_0.

No definitive way of choosing the number of flavor exists in this formalism. It is unclear whether the total number of flavor or the number suitable to a particular quark system should be used. Therefore, we consider three possibilities: (1) N_f = number of flavor = 3, (2) $N_f=6$, and (3) dividing the momentum space into $N_f=2$–6 regions. In the third case, the two constants in the expression for $\tilde\alpha(q^2)$ are determined by continuity of $\tilde\alpha(q^2)$ and $\tilde\alpha'(q^2)$ at the region boundaries. All cases have similar results and there is no conclusive way to choose among them in the χ, Υ range.

III. DETERMINATION OF THE POTENTIAL

To determine the potential, we must determine the parameters in the equation

$$V(r)=\tfrac{2}{3}Ar-\frac{2}{3}\frac{2\pi}{b_1\ln(ke^{-\mu r}/r+d)}\frac{1}{r}. \tag{3.1}$$

For $N_f=3$, we call $\alpha(2\text{ GeV})/2\pi=0.085$ and 0.075 cases 1a and 1b, respectively. Then, Eqs. (2.8), (2.5), and either the experimental result $\alpha(2\text{ GeV})/2\pi=0.085$ (case 1a) or 0.075 (case 1b) are used to calculate α_0 and Λ. Also, b_1 and b_2 depend on the number of flavors assumed. These parameters are given in Table I. As mentioned above, parameters μ and k are determined from the Fourier integral of $\tilde{\alpha}(q^2)/q^2$ at $r=0.5$ and $r=2.0$. The graphs of $\tilde{\alpha}(q^2)$ in these cases are shown in Fig. 1.

In case 1a $[\alpha(2\text{ GeV})/2\pi=0.085]$, the potential is given by

$$V(r)=0.1768r-\frac{0.9308}{\ln[(0.6962/r)e^{-0.1120r}+1.9228]}\frac{1}{r} \tag{3.2}$$

(we use GeV units here and subsequently). In case 1b $[\alpha(2\text{ GeV})/2\pi=0.075]$, the potential is given by

$$V(r)=0.1768r-\frac{0.9308}{\ln(1.216e^{-0.5799r}/r+2.495)}\frac{1}{r}. \tag{3.3}$$

Potentials for the cases 1a and 1b are shown in Fig. 2.

In case 2 ($N_f=6$), the procedure for 1a $[\alpha(2\text{ GeV})/2\pi=0.085]$ resulted in $C\simeq 0$ [C is given in Eq. (2.12)]. Instead of this procedure, we impose the condition $C=0$ to obtain α_0 and Λ. As in the previous cases, a numerical integration of $\tilde{\alpha}(q^2)$ from Eqs. (2.5) and (2.6) is used to calculate μ and k. Relevant parameters are shown in Table I. The potential form is then

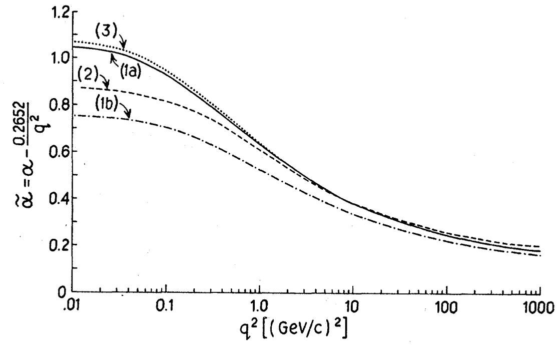

FIG. 1. The function $\tilde{\alpha}(q^2)=\alpha(q^2)-A/q^2$. Case 1a: $N_f=3$ and $\alpha(2\text{ GeV})/2\pi=0.085$; case 1b: $N_f=3$ and $\alpha(2\text{ GeV})/2\pi=0.075$; case 2: $N_f=6$ and $\alpha(2\text{ GeV})/2\pi=0.085$; case 3: $N_f=2$–6 (or 0–6) and $\alpha(2\text{ GeV})/2\pi=0.085$.

$$V(r)=0.1768r-\frac{1.197}{\ln[(1.226/r)e^{-0.5546r}+3.059]}\frac{1}{r}. \tag{3.4}$$

The graphs of $\tilde{\alpha}(q^2)$ and $V(r)$ in this case are shown in Figs. 1 and 2, respectively. Note that, with $C=0$, the interpolated form of $\tilde{\alpha}(q^2)$ may be approximated by

$$\tilde{\alpha}(q^2)=\frac{4\pi}{b_1\ln(a+bq^4)}. \tag{3.5}$$

In case 3, the division of the flavor regions in momentum space was determined by the thresholds for new quarks and the assumption that the ratios of successive quark masses is constant. The choice of region boundaries is then

$N_f=2$, $q^2<1.85$,

$N_f=3$, $1.85<q^2<13.6$,

$N_f=4$, $13.6<q^2<100$,

$N_f=5$, $100<q^2<735$,

$N_f=6$, $735<q^2$.

With the condition $\alpha(2\text{ GeV})/2\pi=0.085$ and continuity of $\tilde{\alpha}$ and $\tilde{\alpha}'$ at the boundaries, we obtain the following formulas:

TABLE I. Parameters for cases 1, 2 in GeV units. The underlined quantities are input.

N_f	b_1	b_2	$\frac{\alpha(2\text{ GeV})}{2\pi}$	$\frac{\alpha_0}{2\pi}$	Λ	B	d	μ	k
3	$\frac{9}{2}$	16	$\underline{0.085}$	0.0295	0.65	1.068	1.923	0.1120	0.6962
			$\underline{0.075}$	0.0562	0.466	0.7636	2.495	0.5799	1.216
6	$\frac{7}{2}$	$\frac{13}{2}$	0.0865	0.1032	0.376	0.8027	3.059	0.5546	1.226

$$q^2<1.85\,,\quad q^2=\frac{0.2652}{\alpha}e^{1.3000/\alpha}\left(1+\frac{0.1133}{\alpha}\right)^{-1.8205},$$

$$1.85<q^2<13.6\,,\quad q^2=\frac{0.2731}{\alpha}e^{1.3963/\alpha}\left(1+\frac{0.1951}{\alpha}\right)^{-1.7901},$$

$$13.6<q^2<100\,,\quad q^2=\frac{0.3452}{\alpha}e^{1.508/\alpha}\left(1+\frac{0.4087}{\alpha}\right)^{-1.7392},$$

$$100<q^2<735\,,\quad q^2=\frac{8.250}{\alpha}e^{1.6391/\alpha}\left(1+\frac{6.136}{\alpha}\right)^{-1.6578}\simeq 0.3834\,e^{1.6391/\alpha}\,\alpha^{0.6578},$$

$$q^2>735\,,\quad q^2\simeq 0.1359\,e^{1.7952/\alpha}\,\alpha^{0.5306}.$$

The function $\tilde{\alpha}(q^2)$ obtained in case 3 is very similar to that in case 1a. Deviation of a few percent from case 1a occurs only at small q^2 as can be seen in Fig. 1. The parameters k and μ in (3.1) are fixed by the same method used in cases 1a and 1b. The resulting potential is

$$V(r)=0.1768r-\frac{1.197}{\ln[(1.028/r)e^{-0.4179r}+2.272]}\,\frac{1}{r}\,. \quad (3.6)$$

Case 3, as reflected in (3.6), corresponds to massless up and down quarks because we assume $N_f(q^2=0)=2$. The assumption that $N_f(q^2=0)=0$, corresponding to nonzero up and down quark mass, alters the function $\tilde{\alpha}(q^2)$ in the region $0<q^2<0.25$. The change in the potential is not large and the result is

$$V(r)=0.1768r-\frac{1.197}{\ln[(1.182/r)e^{-0.1112r}+2.245]}\,\frac{1}{r}\,. \quad (3.7)$$

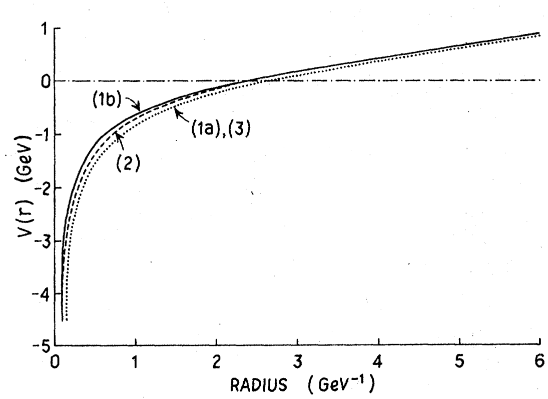

FIG. 2. Potentials. Case 1a: $N_f=3$ and $\alpha(2\text{ GeV})/2\pi=0.085$ [Eq. (3.2)]; case 1b: $N_f=3$ and $\alpha(2\text{ GeV})/2\pi=0.075$ [Eq. (3.3)]; case 2: $N_f=6$ and $\alpha(2\text{ GeV})/2\pi=0.085$ [Eq. (3.4)]; case 3: $N_f=0$–6 and $\alpha(2\text{ GeV})/2\pi=0.085$ [Eq. (3.7)].

We use Eq. (3.7) for our analysis instead of (3.6). Because the dependence of the potential on $\tilde{\alpha}$ in this region ($0<q^2<0.25$) is small, we determine the parameter B by extrapolation from previous cases.

IV. COMPARISON WITH EXPERIMENTAL DATA

With each of the potentials we calculate energy spectrum, leptonic decay width, and $1P-2S$, $1S$ $E1$ transition rates. For the leptonic decay width we use the Van Royen–Weisskopf[14] formula

$$\Gamma(V\to l\bar{l})=\frac{16\pi e_q^2\alpha^2}{M_V^2}|\psi_V(0)|^2\,, \quad (4.1)$$

where M_V = triplet S-state resonance mass. The $E1$ transition rate is calculated using

$$\Gamma(n^3S_1\to n'^3P_J+\gamma)=\tfrac{4}{3}\alpha\omega^3e_q^2\,\frac{(2J+1)}{9}\left(\int_0^\infty R_{n0}R_{n'1}r^3dr\right)^2 \quad (4.2)$$

and

$$\Gamma(n'^3P_J\to n'S_0+\gamma)=\tfrac{4}{9}\alpha\omega^3e_q^2\left(\int_0^\infty R_{n0}R_{n'1}r^3dr\right)^2. \quad (4.3)$$

It is assumed that $e_q=-\frac{1}{3}$ for Υ and $\frac{2}{3}$ for ψ. In Eq. (4.2) the experimental values of ω are used, although a complete theory would include L-S coupling to derive the P-state energy splitting. The results of these calculations are given in Tables II–V for the potentials discussed in Sec. III. In Table VI we have the experimental data[15] for Υ and ψ.

An examination of the calculations and experimental data reveals the following:

(1) All potentials examined have essentially the same results. Variation of $\alpha(2\text{ GeV})/2\pi$ within experimental error has little effect on predictions of ψ and Υ data. Also, varying the number of flavor has little effect on either potential form or ψ, Υ data prediction.

TABLE II. Results of calculations for case 1a, with quark reduced mass (QRM) = 2.0 GeV (Υ) and QRM = 1.0 GeV (ψ). The underlined quantities are input.

E_{ns} (GeV)	Υ	ψ	E_n (GeV)	Υ	ψ	E_{nD} (GeV)	Υ	ψ
E_{1S}	$\underline{9.46}$	$\underline{3.10}$	E_{1P}	10.01	3.63	E_{1D}	10.33	3.97
E_{2S}	10.17	3.81	E_{2P}	10.46	4.12	E_{2D}	10.69	4.37
E_{3S}	10.58	4.27	E_{3P}	10.80	4.51	E_{3D}	10.98	4.72
E_{4S}	10.91	4.65	E_{4P}	11.08	4.85	E_{4D}	11.24	5.03

Leptonic decay width (keV)	Υ	ψ	$E1$ transition rate (keV)	Υ	ψ
1S	1.67	18.92	$2S-1^3P_0$	6.55	47.57
2S	0.691	6.85	$2S-1^3P_1$	5.09	37.0
3S	0.478	4.36	$2S-1^3P_2$	3.91	28.45
4S	0.384	3.28	1^3P_0-1S	40.48	347
			1^3P_1-1S	92.84	795
			1^3P_2-1S	122.1	1049

(2) We have obtained satisfactory results for the Υ spectrum and leptonic decay rate. For example, in case 1b we calculate a $1S$-$2S$ energy split of).62 GeV and a leptonic decay width of 1.81 keV as compared with experimental values of 0.6 GeV nd 1.3 ± 0.4 keV, respectively. Notice that the nodels essentially contain no free parameters, lthough the Υ quark mass was assumed to be ither 2.0 or 2.5 GeV depending on the results. A lear test of the models will be possible when there are more experimental data on Υ. This is forthcoming in the PETRA and PEP experiments.

(3) The results of the ψ spectrum and ratios of the leptonic decay widths of triplet S excited states are in fair agreement with experiment. However, the absolute values of the leptonic decay widths and the $E1$ transition rates to 1^3P_J states are 2–3 times larger than experimental results. This problem has been encountered with other potentials.[1-6]

TABLE III. Results of calculations for case 1b, with QRM = 2.5 GeV (Υ) and QRM = 1.0 GeV (ψ). The underlined quantitites are input.

E_{nS} (GeV)	Υ	ψ	E_{nP} (GeV)	Υ	ψ	E_{nD} (GeV)	Υ	ψ
E_{1S}	$\underline{9.46}$	$\underline{3.10}$	E_{1P}	9.94	3.57	E_{1D}	10.23	3.88
E_{2S}	10.08	3.75	E_{2P}	10.35	4.04	E_{2D}	10.56	4.28
E_{3S}	10.45	4.19	E_{3P}	10.67	4.42	E_{3D}	10.83	4.61
E_{4S}	10.75	4.55	E_{4P}	10.93	4.75	E_{4D}	11.07	4.92

Leptonic decay width (keV)	Υ	ψ	$E1$ transition width (keV)	Υ	ψ
$1S$	1.81	14.41	$2S-1^3P_0$	5.75	49.33
$2S$	0.815	4.98	$2S-1^3P_1$	4.48	38.39
$3S$	0.576	3.61	$2S-1^3P_2$	3.44	29.50
$4S$	0.469	2.85	1^3P_0-1S	37.61	395.6
			1^3P_1-1S	86.20	908.2
			1^3P_2-1S	113.7	1197

TABLE IV. Results of calculations for case 2, with QRM = 2.0 GeV (Υ) and QRM = 1.0 GeV (ψ). The underlined quantities are input.

E_{nS} (GeV)	Υ	ψ	E_{nP} (GeV)	Υ	ψ	E_{nD} (GeV)	Υ	ψ
E_{1S}	$\underline{9.46}$	$\underline{3.10}$	E_{1P}	10.01	3.62	E_{1D}	10.33	3.94
E_{2S}	10.16	3.80	E_{2P}	10.45	4.10	E_{2D}	10.67	4.34
E_{3S}	10.57	4.25	E_{3P}	10.78	4.48	E_{3D}	10.96	4.68
E_{4S}	10.88	4.65	E_{4P}	11.05	4.81	E_{4D}	11.22	5.00

Leptonic decay width (keV)	Υ	ψ	$E1$ transition rate (keV)	Υ	ψ
1S	1.72	19.01	$2S-1^3P_0$	6.79	49.34
2S	0.708	8.85	$2S-1^3P_1$	5.28	38.38
3S	0.487	4.46	$2S-1^3P_2$	4.07	29.52
4S	0.394	3.31	1^3P_0-1S	39.32	347.03
			1^3P_1-1S	90.14	795.38
			1^3P_2-1S	118.91	1049

(4) The 1S-2S energy split, given in Fig. 3, is slowly varying with quark mass in the range $1.0 < \mathrm{QRM} < 6.0$ GeV (QRM = quark *reduced* mass). This behavior resembles that of the logarithmic potential[2,3] in this range (for the logarithmic potential the excitation energy is independent of quark mass). The increase of energy difference for large mass is characteristic of asymptotically free potentials. In the large mass region we would expect $\Delta E \propto m\alpha^2 \propto m/(\ln m)^2$.

(5) Our analytic form for the potential is consistent with Celmaster and Henyey's calculation,[5] which was obtained numerically from Eq. (2.5). We are also in agreement with the mass dependence of the excitation energy drawn in Fig. 3. (Note, however, that Celmaster and Henyey used $\Lambda = 0.5$, whereas our value is 0.466 for the calculations in Fig. 3.) This indicates that the potential (3.1), which exhibits the correct behavior at $r \to 0$ and $r \to \infty$, is a good approximation to the QCD

TABLE V. Results of calculations for case 3, with QRM = 2.0 GeV (Υ) and QRM = 1.0 GeV (ψ). The underlined quantities are input.

E_{nS} (GeV)	Υ	ψ	E_{nP} (GeV)	Υ	ψ	E_{nD} (GeV)	Υ	ψ
E_{1S}	$\underline{9.46}$	$\underline{3.10}$	E_{1P}	10.01	3.63	E_{1D}	10.34	3.97
E_{2S}	10.17	3.82	E_{2P}	10.45	4.12	E_{2D}	10.7	4.38
E_{3S}	10.58	4.28	E_{3P}	10.79	4.52	E_{3D}	10.99	4.73
E_{4S}	10.91	4.65	E_{4P}	11.08	4.85	E_{4D}	11.26	5.04

Leptonic decay width (keV)	Υ	ψ	$E1$ transition rate (keV)	Υ	ψ
1S	1.76	19.01	$2S-1^3P_0$	6.63	47.57
2S	0.723	7.01	$2S-1^3P_1$	5.16	37.00
3S	0.499	4.50	$2S-1^3P_2$	3.96	28.43
4S	0.400	3.37	1^3P_0-1S	38.67	346.9
			1^3P_1-1S	88.63	795.3
			1^3P_2-1S	116.9	1048

TABLE VI. Experimental data.

E_{nS} (GeV)	Υ	ψ	Leptonic decay width (keV)	Υ	ψ
E_{1S}	9.46 ± 0.01	3.097 ± 0.002	1S	1.3 ± 0.4	4.7 ± 0.7
E_{2S}	10.01 ± 0.01	3.686 ± 0.003	2S	0.32 ± 0.10	2.1 ± 0.2
E_{3S}			3S	0.5 ± 0.2	
E_{4S}			4S		
E_{5S}		4.414 ± 0.007	5S		0.43 ± 0.13

$E1$ transition rate (GeV)	Υ	ψ	L-S splitting $1P_J$ states (GeV)	ψ
$2\,^3S_1$-$1\,^3P_0$		16 ± 9	$1\,^3P_2$	3.55
$2\,^3S_1$-$1\,^3P_1$		16 ± 9	$1\,^3P_1$	3.51
$2\,^3S_1$-$1\,^3P_2$		16 ± 9	$1\,^3P_0$	3.41

potential. (The QCD potential is defined as the potential resulting only from considerations of Sec. II.)

(6) The results of (2) and (3) may be understood with the expectation that Υ is a nonrelativistic system whereas the relativistic correction for ψ may be significant. A proper treatment of relativistic effects in these systems is needed to resolve the discrepancies. The effect of opening decay channels, as analyzed in Ref. 1, may also account for part of the discrepancies.

V. THE SPIN-SPIN INTERACTION

Recent experiments[15] have established a state for ψ at 2.85 GeV which is likely to be a singlet $^1S_0$ state. This indicates a spin-spin splitting of 250 MeV. It has been pointed out[16] that the spin-spin interaction due to relativistic effects is not sufficient to account for this splitting. Recently, it has been suggested[8] that instantons could be a source of a large spin-spin interaction.

In order to see how this interaction could modify

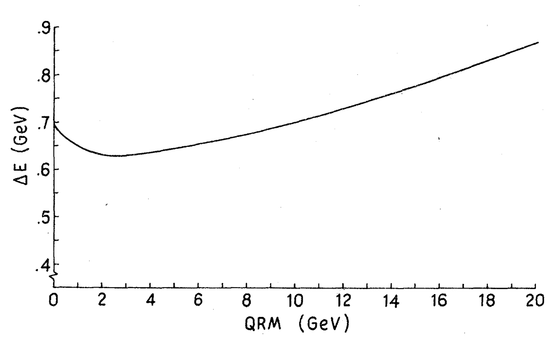

FIG. 3. $2S$–$1S$ energy difference as a function of quark reduced mass (QRM).

the leptonic decay rate, consider $V=(V_{\mathrm{QCD}} + V_s\vec{s}_1\cdot\vec{s}_2)$. For simplicity, assume a square-well–type potential $V_s = V_0\theta(b-r)$, where $V_0>0$ for the correct spin-spin splitting. Define the S state $\psi = 1/\sqrt{4\pi}\,u(r)/r$, then

$$[u'(0)]^2 = 2m\left\langle\frac{dV}{dr}\right\rangle = 2m\left\langle\frac{dV_{\mathrm{QCD}}}{dr}\right\rangle - 2m\langle\vec{s}_1\cdot\vec{s}_2\,V_0\,\delta(b-r)\rangle\,. \tag{5.1}$$

Assuming a short range ($b\ll1$) for the instanton interaction we have

$$[u'(0)]^2 = 2m\left\langle\frac{dV_{\mathrm{QCD}}}{dr}\right\rangle - \frac{m}{2}V_0 b^2[u'(0)]^2\,,\quad \text{for } {}^3S_1$$

and (5.2)

$$[u'(0)]^2 = 2m\left\langle\frac{dV_{\mathrm{QCD}}}{dr}\right\rangle + \frac{3m}{2}V_0 b^2[u'(0)]^2\,,\quad \text{for } {}^1S_0\,.$$

Also,

$$2m\left\langle\frac{dV_{\mathrm{QCD}}}{dr}\right\rangle \cong [u'_{\mathrm{QCD}}(0)]^2$$

implies

$$[u'(0)]^2 = \frac{[u'_{\mathrm{QCD}}(0)]^2}{(1+mV_0b^2/2)}\,,\quad \text{for } {}^3S_1$$

and (5.3)

$$[u'(0)]^2 = \frac{[u'_{\mathrm{QCD}}(0)]^2}{(1-3mV_0b^2/2)}\,,\quad \text{for } {}^1S_0\,.$$

This indicates that the leptonic width of the triplet S state is decreased and that of the singlet S state is increased. Notice also that the ratio of the leptonic decay widths between various triplet S states in the total solution is the same as those of the QCD calculations. This may not be true for the correct instanton potential, however, qualitative features will probably be retained.

A serious problem with the spin-spin interaction due to relativistic effects appears in calculating the wave function at the origin. In the case of positronium calculations, such interactions contained a δ function which can be successfully applied to energy shift calculations. The perturbational correction to the wave function due to a potential $\delta^3(\vec{r})$ has a singular term at the origin and therefore has no meaning. The trouble may be traced to the neglect of other relativistic correction terms, such as p^4. In order to resolve this problem, a more complete understanding of the relativistic correction is needed.

We will report in more detail an effect of spin-spin interaction in the future.

Notes added. (1) In order to obtain the confinement part of the potential we probably have to consider the effect of multiple-gluon exchange. This necessitates a modification of the underlying assumptions of our approach. However, we show below that the potential form (3.1) remains intact.

We define $\alpha_T(q^2)/q^2$ as the Fourier transform of the potential and write $\alpha_T(q^2)=\alpha(q^2)+\alpha_1(q^2)$ where $\alpha(q^2)$ is the running coupling constant and $\alpha_1(q^2)$ represents multigluon exchange contribution.

Asymptotic freedom would imply $\alpha_T(q^2)\to\alpha(q^2)\to 2\pi/b_1\ln q^2$ (2.19) as $q^2\to\infty$. The confinement assumption would imply $\alpha_T(q^2)\to A/q^2$ as $q^2\to 0$. An argument similar to that in Sec. II can be applied to $\alpha_T(q^2)$ instead of $\alpha(q^2)$ and leads to an analytic form for $\alpha_T(q^2)$. By the argument in the Appendix our analytic form for the potential is dependent only on the branch cuts of α_T in the complex q plane. Thus we obtain Eq. (3.1), but lose predictive power of parameters μ, k, and d. An analysis of the two-gluon exchange contribution to $\alpha_T(q^2)$ may lead to a prediction of parameter d. From this point of view, we feel that more extensive use of experimental data is necessary with potential (3.1). The authors are indebted to B. Sakita for criticism and discussion on this point.

(2) After submitting this paper, we came across articles[18] which suggest that the Van Royen–Weisskopf formula should be modified by radiative correction. This would be another mechanism which suppresses the value of the leptonic decay rate at least for the low-lying vector particle such as ψ/J.

ACKNOWLEDGMENTS

The authors are indebted to C. K. Lee for useful comments and discussions. This research was supported in part by the U. S. Department of Energy.

APPENDIX: ASYMPTOTIC FORM OF THE FOURIER INTEGRAL (2.6)

Define the integral

$$I=\int_0^\infty \frac{1}{\ln(a+bq^2)}\,\frac{\sin qr}{q}\,dq$$
$$=\int_0^\infty\left(\frac{1}{\ln(a+bq^2)}-\frac{1}{\ln a}\right)\frac{\sin qr}{q}\,dq+\frac{\pi}{2\ln a}\,. \tag{A1}$$

Consider,

$$J=\int_{-\infty}^{+\infty}\left(\frac{1}{\ln(a+bq^2)}-\frac{1}{\ln a}\right)\frac{e^{iqr}}{q}\,dq\,, \tag{A2}$$

then

$$I(r)=[\tfrac{1}{2}\,\mathrm{Im}\,J+(\pi/2)\,1/\ln a]\,. \tag{A3}$$

In order to evaluate J, we use contour C shown in Fig. 4 (with $r>0$) and define

$$F=\frac{1}{\ln(a+bq^2)}\,\frac{e^{iqr}}{q}\,. \tag{A4}$$

With the branch cuts of the logarithm shown in the figure, we must evaluate the discontinuity of F across the cut. Then

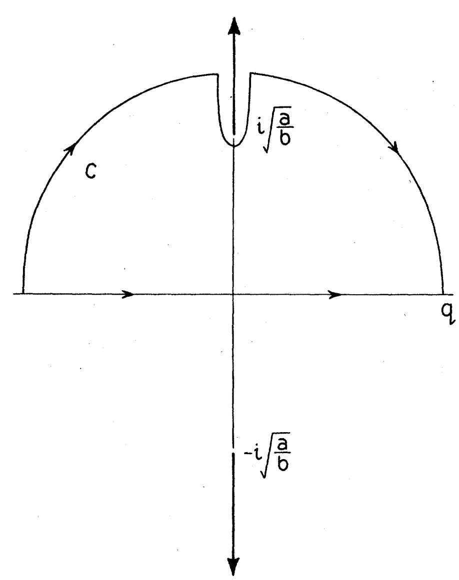

FIG. 4. Contour of integration (A2).

$$[(F)_{q=ix+\epsilon}-(F)_{q=ix-\epsilon}]=\frac{-2\pi e^{-xr}}{x\{[\ln(bx^2-a)]^2+\pi^2\}} \tag{A5}$$

and integrating around the contour yields

$$J=-2\pi i\int_{\sqrt{a/b}}^{\infty}\frac{e^{-xr}}{x}\,\frac{dx}{x\{[\ln(bx^2-a)]^2+\pi^2\}}\,. \tag{A6}$$

Let $x=\sqrt{a/b}+t$, then

$$J=-2\pi i e^{-(\sqrt{a/b})r}\times\int_0^{\infty}\frac{e^{-tr}dt}{(t+\sqrt{a/b})(\{\ln b[t^2+2(\sqrt{a/b})t]\}^2+\pi^2)}\,. \tag{A7}$$

We are interested in the asymptotic behavior of the integral (for large r). $J\equiv-2\pi i e^{-(\sqrt{a/b})r}k(r)$, then

$$k(r)\xrightarrow{r\to\infty}\int_0^{\infty}\frac{1}{\sqrt{a/b}}\,\frac{e^{-tr}dt}{[(\ln t)^2+\pi^2]}\to\int_0^{\infty}\frac{1}{\sqrt{a/b}}\,\frac{e^{-tr}(1+t)dt}{[(\ln t)^2+\pi^2]}\,. \tag{A8}$$

This integral was found in standard tables[17]

$$\int_0^{\infty}\frac{dt}{\sqrt{a/b}}\,\frac{e^{-tr}(1+t)}{[(\ln t)^2+\pi^2]}=\frac{1}{\sqrt{a/b}}[\nu'(r)-\nu''(r)]\,, \tag{A9}$$

where

$$\nu(r)\equiv\int_0^{\infty}\frac{r^t dt}{\Gamma(1+t)}\,.$$

We want to estimate $[\nu'(r)-\nu''(r)]$ for large r. We have

$$[\nu'(r)-\nu''(r)]=-\int_{-2}^{-1}\frac{e^{t\ln r}dt}{\Gamma(t+1)} \tag{A9$'$}$$

and integration by parts twice leads to (in limit $r\to\infty$)

$$[\nu'(r)-\nu''(r)]=\frac{-1}{(\ln r)^2}\,\frac{r^t}{\Gamma(t+1)}\,\psi(t+1)\Big|_{t=-2}^{t=-1}+\frac{1}{(\ln r)^2}\int_{-2}^{-1}r^t\left(\frac{\psi(t+1)}{\Gamma(t+1)}\right)dt, \tag{A10}$$

where $\psi(t)=\Gamma'(t)/\Gamma(t)$. Taking the first term and using $\psi(t)/\Gamma(t)\to+1$ for $t\to-1$ and $\psi(t)/\Gamma(t)\to-2$ for $t\to-2$, we have

$$\nu'(r)-\nu''(r)\to\frac{1}{r(\ln r)^2}+O\left(\frac{1}{r(\ln r)^3}\right). \tag{A11}$$

Therefore

$$J\to-2\pi i e^{-\sqrt{a/b}\,r}\sqrt{b/a}\;\frac{1}{r(\ln r)^2} \tag{A12}$$

and

$$I(r)\to\frac{\pi}{2}\,\frac{1}{\ln a}\left(1-\frac{2\ln a\sqrt{b/a}\,e^{-\sqrt{a/b}\,r}}{r(\ln r)^2}\right). \tag{A13}$$

Equation (A13) leads to the asymptotic form (2.18).

It is important to note that the behavior for large r is general in that it can be derived from different forms of $\tilde{\alpha}(q^2)$. This is due to the prominent part of the exponential in the solution which depends only on the branch points of the logarithm. For example,

$$J=\int_{-\infty}^{+\infty}\left[\frac{1}{\ln(a+bq^4)}-\frac{1}{\ln a}\right]\frac{e^{iqr}}{q}dq \tag{A14}$$

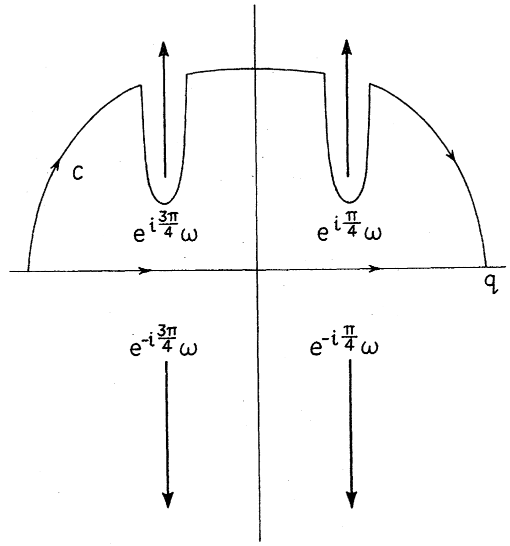

FIG. 5. Contour of integration (A14), $[\omega=(a/b)^{1/4}]$.

is calculated using contour C shown in Fig. 5. Letting $\omega=(a/b)^{1/4}$, we find, after tedious computation of the discontinuity across the branch and a limiting procedure similar to the one above, an asymptotic form

$$J\to\frac{-4\pi}{\omega}\left[\frac{e^{-\omega r/\sqrt{2}}\cos(\omega r/\sqrt{2}+\pi/4)}{r(\ln r)^2}\right]. \tag{A15}$$

In this expression the argument of the exponential is determined by the distance from the x axis to the branch point; a property which is very general. Another example,

$$\tilde{\alpha}(q^2)=\frac{1}{\prod_i\ln(a_i+b_iq^2)}\quad(a_i,\,b_i>0)$$

implies

$$V\xrightarrow{r\to\infty}\left[1-\frac{ke^{-\mu r}}{r(\ln r)^2}\right], \tag{A16}$$

where $\mu=\min_i[(a_i/b_i)^{1/2}]$ and k is a constant.

[1]K. Gottfried, Cornell report, 1978 (unpublished) and other references therein; E. Eichten *et al.*, Phys. Rev. D 17, 3090 (1978). Earlier works on this subject include T. Appelquist *et al.*, Phys. Rev. Lett. 34, 365 (1975); E. Eichten *et al.*, *ibid.* 34, 369 (1975); B. J. Harrington, S. Y. Park, and A. Yildiz, *ibid.* 34, 168 (1975); 34, 706 (1975); J. S. Kang and H. J. Schnitzer, Phys. Rev. D 12, 841 (1975); 12, 2791 (1975).

[2]M. Machacek and Y. Tomozawa, Prog. Theor. Phys. 58, 1890 (1977); Ann. Phys. (N.Y.) 110, 407 (1978); C. Quigg and J. L. Rosner, Phys. Lett. 71B, 153 (1977).

[3]Y. Muraki, Prog. Theor. Phys. 41, 473 (1969); Y. Muraki, K. Mori, and M. Nakagawa, Cosmic Ray Laboratory, Tokyo, report, 1978 (unpublished).

[4]W. Celmaster, H. Georgi, and M. Machacek, Phys. Rev. D 17, 879 (1978).

[5]W. Celmaster and F. Henyey, Phys. Rev. D 18, 1688 (1978).

[6]G. Bhanot and S. Rudaz, Cornell Report No. CLNS-393, 1978 (unpublished); T. Sterling, Nucl. Phys. B141, 272 (1978).

[7]Celmaster and Henyey fit a power form for the potential to their numerical results. Because this does not satisfy the correct asymptotic behavior of the potential, it is not satisfactory.

[8]F. Wilczek and A. Zee, Phys. Rev. Lett. 40, 83 (1978).

[9]F. Feinberg, Phys. Rev. Lett. 39, 316 (1977); T. Appelquist, M. Dine, and I. Muzinich, Phys. Lett. 69B, 231 (1977).

[10]C. G. Callan, Jr., Phys. Rev. D 2 (1970); K. Symanzik, Commun. Math. Phys. 18, 227 (1970).

[11]D. Gross and F. Wilczek, Phys. Rev. Lett. 26, 1343 (1973); H. D. Politzer, *ibid.* 26, 1346 (1973); H. D. Politzer, Phys. Rep. 14 C, 129 (1974); W. E. Caswell, Phys. Rev. Lett. 33, 244 (1974).

[12]This is obtained by analytic continuation of the formula

$$\int_0^\infty dq\,\frac{1}{q^n}\,\frac{\sin qr}{qr}=\frac{\pi}{2}\,r^{n-1}\,\frac{1}{\Gamma(1+n)\cos(n\pi/2)}\,.$$

[13]A. De Rújula, H. Georgi, and H. D. Politzer, Ann. Phys. (N.Y.) 103, 315 (1977); R. Shankar, Phys. Rev. D 15, 755 (1977); R. G. Moorhouse, M. R. Pennington, and G. C. Ross, Nucl. Phys. B124, 285 (1977).

[14]R. Van Royen and V. F. Weisskopf, Nuovo Cimento 50A, 617 (1967).

[15]Particle Data Group, Phys. Lett. 75B (1978); Pluto Collaboration, Observation of a narrow resonance formed in e^+e^- annihilation at 9.46 GeV, DESY, report, 1978 (unpublished); Reports at the XIX International Conference on High Energy Physics, Tokyo, 1978 (unpublished).

[16]For example, T.-M. Yan, in *Quark Confinement and Field Theory*, edited by D. Stump and D. Weingarten (Wiley, New York, 1977).

[17]I. S. Gradshteyn and I. M. Ryzhik, *Tables of Integrals, Series and Products* (Academic, New York, 1965), p. 579.

[18]R. Barbieri, R. Kogerler, Z. Kunszt, and R. Gatto, Nucl. Phys. B105, 125 (1976); W. Celmaster, Phys. Rev. D 19, 1517 (1979).